Layered double hydroxide nanoparticles as cellular delivery vectors of supercoiled plasmid DNA

Zhi Ping Xu[1]
Tara L Walker[2]
Kerh-lin Liu[1]
Helen M Cooper[2]
GQ Max Lu[1]
Perry F Bartlett[2]

[1]ARC Centre for Functional Nanomaterials, Australian Institute of Bioengineering and Nanotechnology; [2]Queensland Brain Institute, The University of Queensland, Brisbane, QLD 4072, Australia

Abstract: We prepared stable homogeneous suspensions with layered double hydroxide (LDH) nanoparticles for in vitro gene delivery tests. The viability of HEK 293T cells in the presence of LDH nanoparticles at different concentrations was investigated. This revealed 50% cell viability at 500 μg/mL of LDH nanoparticles that is much higher than 50–100 μg/mL used for the delivery tests. The supercoiled pEF-eGFP plasmid (*ca*. 6100 base pairs) was mixed with LDH nanoparticle suspensions for anion exchange at a weight ratio of DNA/LDH between 1:25 and 1:100. In vitro experiments show that GFP expression in HEK 293T cells starts in the first day, reaches the maximum levels by the second day and continues in the third day. The GFP expression generally increases with the increase in DNA loading in DNA-LDH nanohybrids. However, the delivery efficiency with LDH nanoparticles as the agent is low. For example, the relative efficiency is 7%–15% of that of the commercial agent FuGENE®6. Three to 6% of total cells expressed GFP in an amount detectable by the FACS cytometry 2 days after transfection at 1 μg/mL of plasmid DNA with 25 μg/mL of LDH nanomaterial. The lower delivery efficiency could be attributed to the aggregation of LDH nanoparticles caused by the long-chain plasmid DNA.

Keywords: layered double hydroxide, nanoparticles, gene delivery, nonviral vectors, cytotoxicity

Introduction

Over the past few decades, scientists have been searching for suitable gene delivery systems to realize the dream of overcoming human genetic diseases. Many types of nonviral vectors (Pouton and Seymour 1998; Luo and Saltzman 2000; Dietz and Bahr 2004; Leong 2005; Xu et al 2006a), including liposomes, cationic polymers (Pouton and Seymour 1998; Luo and Saltzman 2000; Leong 2005), recombinant proteins (Dietz and Bahr 2004) and inorganic nanoparticles (Xu et al 2006a), have been widely investigated. However, their clinical applications have been limited by the inefficiency in a few consecutive processes: cellular uptake, release of the gene from the endosome, and nuclear targeting and transport (Khalil et al 2006; van der Aa et al 2006). It is expected that advances in nanoscale materials sciences, such as the control of particle size and shape, the variety of the particle surface properties, the proper fusion of DNA fragment with the nanoparticles and the suitable release of DNA from the particles will overcome these barriers, leading to higher-efficiency DNA delivery (Xu et al 2006a). Currently, the design of safe and efficient gene delivery systems remains one of the key challenges in gene therapy (Nielsen 2005).

In recent years, increasing efforts worldwide have been devoted to developing various inorganic materials as novel nonviral delivery systems (Barbe et al 2004; Xu et al 2006a). This is due to the recognition that inorganic nanoparticles generally possess versatile properties suitable for gene delivery, including wide

Correspondence: GQ Max Lu
ARC Centre for Functional Nanomaterials, Australian Institute of Bioengineering and Nanotechnology, The University of Queensland, Brisbane, QLD 4072, Australia
Tel +61 7 3365 3885
Fax +61 7 3365 6074
Email maxlu@uq.edu.au

availability, rich functionality, good biocompatibility, potential capability of target delivery and controlled release of carried genes. Amongst these, layered double hydroxide nanomaterial appears to be an outstanding candidate.

LDHs are a group of anion-exchanging materials containing mixed metal hydroxides similar to brucite, $Mg(OH)_2$. In a brucite layer, each Mg^{2+} ion is octahedrally surrounded by six OH^- ions and the different octahedra share edges to form an infinite 2D layer. In hydrotalcite $[Mg_6Al_2(OH)_{16}][CO_3 \cdot 4H_2O]$, the replacement of Mg^{2+} by Al^{3+} gives the brucite-like layer positive charges that are balanced by carbonate anions located in the interlayer region. The positively charge brucite-like layers ($[Mg_6Al_2(OH)_{16}]^{2+}$), interlayer anions as well as water molecules ($[CO_3 \cdot 4H_2O]^{2-}$) are held together via electrostatic interactions and hydrogen bonds to form a 3D structure (Cavani et al 1991; Braterman et al 2004). In general, LDHs can be chemically expressed by a formula like $[M^{2+}_{1-x}M^{3+}_x(OH)_2]^{x+}[(A^{m-})_{x/m} \cdot nH_2O]^{x-}$, where M^{2+} can be most divalent cations such as Mg, Zn, Ni, Co, and Fe, M^{3+} most trivalent cations such as Al, Fe, and Cr, and A^{m-} the exchangeable anions, such as $CO_3^{2-}, Cl^-, SO_4^{2-}$, various organic anions and complex anions.

LDHs can be readily synthesized in the laboratory with controllable lateral size between 40 and 300 nm (Xu et al 2006b). A number of experiments have been reported involving the intercalation (loading) of nucleotides, oligonucleotides and genes into the LDH interlayer (Choy et al 1999, 2000; Kriven et al 2004; Desigaux et al 2006), the cytotoxicity of LDH materials to the cells (Kriven et al 2004; Tyner et al 2004), the cellular uptake of LDH nanoparticles (Choy et al 2000, 2001; Tyner et al 2004), and the in vitro gene transfection tests in different cell lines (Choy et al 2000; Tyner et al 2004) as well as target delivery by conjugating the antibody protein (Tyner et al 2004). These investigations indicate that LDH nanomaterial could be used as an effective gene delivery system. In advancing this expectation, we prepared Mg_2Al-Cl-LDH nanoparticles in 50–300 nm with a regularly hexagonal platelet shape, loaded a pEF-eGFP plasmid (*ca*. 6100 base-pairs) to LDH nanoparticles, and transfected a mammalian cell line (HEK 293T) in vitro. We have also re-examined the cytotoxicity of Mg_2Al-Cl-LDH nanoparticles in this paper. The observations show that LDH nanoparticles can be used as a potential nonviral delivery system, but need further optimization to enhance the delivery efficiency.

Materials and methods

Preparation of LDH nanoparticle suspensions

Layered double hydroxides (LDHs) were prepared by co-precipitation and subsequent hydrothermal treatment. In brief, the pristine $Mg_2Al(OH)_6Cl \cdot 1.5H_2O$ was prepared by quickly adding 10 mL of mixed salt solution containing $MgCl_2$ (3.0 mmol) and $AlCl_3$ (1.0 mmol) (within 5 seconds) into 40 mL of NaOH solution (0.15 M, just enough for forming Mg_2Al-LDH) to coprecipitate under vigorous stirring, followed by 10-minute stirring with the reactor isolated from air (Boclair and Braterman 1999; Xu et al 2006b). The $Mg_2Al(OH)_6Cl \cdot 1.5H_2O$ slurry was obtained via centrifuge separation, followed by washing twice with deionized water. The washed slurry was then manually dispersed in 40 mL of deionized water and transferred into a stainless steel autoclave with a Teflon lining. The autoclave was then placed in a pre-heated oven and heated at 100 °C for 16 hours to give rise to a stable homogeneous LDH suspension after air-cooling. As-obtained LDH suspension generally contains hexagonal sheet-like nanoplates with an approximate composition of $Mg_2Al(OH)_6(Cl) \cdot 1.5H_2O$ at a concentration of *ca*. 0.4 wt%. LDH suspensions with *ca*. 0.8 wt% and *ca*. 0.2 wt% were also prepared in the similar way. The pH of 8.5 in such suspensions was normally adjusted to 7.5 by adding one volume of sterile salt solution (2 mM $MgCl_2$ and 1 mM $AlCl_3$) into three volumes of LDH suspensions.

DNA-LDH nanohybrids

The supercoiled pEF-eGFP plasmid was prepared using the Qiagen maxiprep kit and diluted in deionized water at a final concentration of 1 μg/μL. The DNA:LDH weight ratio in the DNA-LDH nanohybrid suspensions was fixed at 1:25, 1:50 or 1:100. For example, to make DNA-LDH suspesnion with DNA:LDH weight ratio of 1:50, 100 μL of LDH suspension (0.80 wt%), 16 μL of plasmid DNA (1 μg/μL), 50 μL of sterile water and 34 μL of sterile Mg-Al buffer solution were mixed and shaken at 37 °C for 4 hours in a sealed sterile tube.

Cell culture and cytotoxicity assay

Human Embryonic Kidney (HEK 293T) cells were cultured in RPMI 1640 growth medium (Invitrogen) supplemented with 10% Fetal Calf Serum (FCS), 100000 U/L penicillin and 50 mg/L streptomycin. In a typical cytotoxicity assay, HEK 293T cells were seeded in 6-well plates at a density of 100,000 cells in 3.0 mL growth medium per well and allowed

to incubate overnight at 37 °C in the atmosphere of 5% CO_2. After 24-hour incubation, the medium was removed and replaced with 3.0 mL of the fresh growth medium containing various amounts of LDH nanomaterial, eg, from 25 to 2000 μg/mL. A control experiment was performed without LDH under the same conditions. After 48 hours of incubation, cells were collected and stained with Trypan Blue, and the live cells were counted using a hemocytometer under Olympus CKX31 microscope. Cell viability was then calculated as the percentage of the live cell number N_{test} over the number $N_{control}$ in the control experiment, ie, $N_{test}/N_{control} \times 100$. The tests were performed in triplicate.

Delivery test and FACS analysis

HEK 293T cells were seeded in 6-well plates at a density of 100,000 cells per well and allowed to incubate at 37 °C in the atmosphere of 5% CO_2 for 24 hours. The growth medium was then removed and replaced with 3.0 mL of fresh growth medium that contained a certain amount of DNA-LDH nanohybrids. After 1-, 2-, or 3-day incubation, cells were imaged using a fluorescence microscope (Olympus IX 81). The cells in each well were then harvested by trypsinization and resuspended to a final volume of 1.0 mL phosphate-buffered saline. Cells in the suspension were sorted by the flow cytometry (λ = 530 nm) on a BD™ LSRII FACS (Fluorescence activated cell sorting) Analyzer, and a total of 30,000 cells were counted for each sample for statistical analysis. The commercial transfection agent FuGENE®6 (Roche) was used in parallel with the above delivery tests.

Characterization

Photon correlation spectroscopy (PCS, Nanosizer Nano ZS, MALVERN Instruments) was used to analyze the particle size distribution from 0.6 to 6000 nm and Zeta potential from –200 to 200 mV of the LDH suspensions, in which the peak positions as well as the polydispersion index (PDI) were automatically calculated. The transmission electron microscopic images were obtained on a JEOL JSM-2010 transmission electron microscope (TEM) at an acceleration voltage of 200 kV. STEM (scanning transmission electron microscopy) images and EDS (energy dispersive X-ray spectrometry) spectra were recorded in a Philips Tecnai 20 FEG analytical electron microscope. For TEM and STEM imaging, the freshly collected LDH nanoparticles were dispersed in alcohol with ultrasonication for 20 min and then a droplet was dropped on a copper grid coated with carbon film. X-ray diffraction patterns were measured for LDH materials collected via high-speed centrifugation at a scanning rate of 1.2° per minute from $2\theta = 5°$ to $2\theta = 75°$ with Co K_α radiation (λ = 0.17902 nm) on a Rigaku Miniflex X-ray diffractometer with a variable slit width. Infrared spectra were collected on a Perkin-Elmer 2000 FTIR after 40 scans within 4000–400 cm^{-1} at a resolution of 4 cm^{-1} by measuring the IR absorbance of KBr disc that contains 1–2 wt% of sample. In addition, the metal contents of suspension samples were determined by inductively coupled plasma and atomic emission spectroscopy (ICP-AES) on a Varian Vista Pro.

Results and discussion

Pristine LDH nanoparticle suspensions

The LDH suspensions visually look very transparent and homogeneous. The pristine LDH materials collected from the suspensions via high-speed centrifugation have the typical layered features, as reflected by the X-ray diffraction pattern in Figure 1. Very sharp and strong diffractions from planes (003) and (006) demonstrate an ordered layer stacking. The interlayer spacing is 0.7633 nm and lattice parameter a is 0.3046 nm for the pristine LDH (Mg_2Al-Cl-LDH), quite similar to those reported elsewhere (Cavani et al 1991; Boclair and Braterman 1999).

Similarly, the FTIR spectrum in Figure 2 is typical of Mg_2Al-LDH materials, as featured by a broad band at 3450 cm^{-1} (ν_{OH}), a weak peak at 1620 cm^{-1} (δ_{H_2O}), bands at 678 and 447 cm^{-1} (due to M-O vibrations and M-O-H bending). The weak peak at 1365 cm^{-1} is due to the stretching vibration of CO_3^{2-} that is converted from CO_2 captured from air during washing) (Hernandez-Morento et al 1985; Nakamoto 1997; Xu and Zeng 2001). In particular, the sharp peak at 447 cm^{-1} and the shoulder over 3450 cm^{-1} are the evidences of Mg_2Al-LDH (Hernandez-Morento et al 1985; Xu and Zeng 2001). Elemental analysis gives the atomic ratio [Mg]/[Al] close to 1.9, slightly less than the designed value (2.0), attributed to more Mg^{2+} leaching than Al^{3+} from the hydroxide layers during the hydrothermal treatment (Xu et al 2006b). The leaching of Mg^{2+} may lead to formation of traces of gibbsite and brucite, as marked with # and ∗ in Figure 1, respectively.

The stable homogeneous Mg_2Al-Cl-LDH suspension typically has a narrow particle size distribution, centred at an average hydrodynamic diameter of *ca*. 122 nm and a narrow zeta potential distribution at *ca*. 39.4 mV (Figure 3). The hydrodynamic particle diameter is exclusively falling in the range of 40–400 nm and 95% in 50–300 nm, with a polydispersion index (PDI) of 0.12. The TEM image in Figure 4 shows that the pristine LDH nanoparticles are well shaped hexagonally as usual (Cai et al 1994), with the lateral

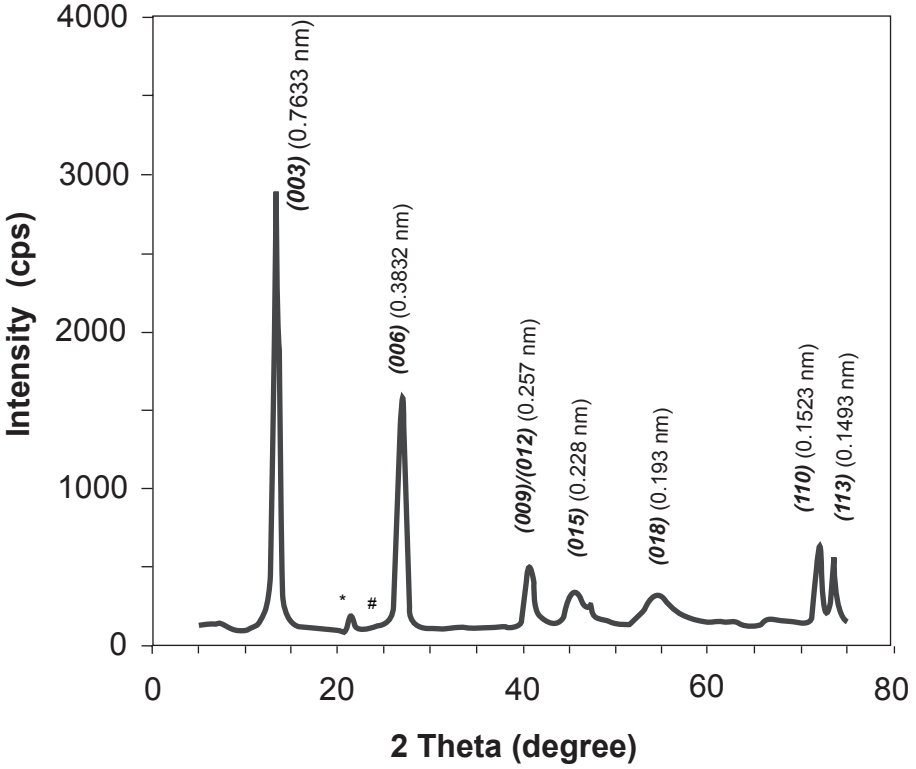

Figure 1 XRD pattern of pristine Mg_2Al-Cl-LDH nanomaterials.
Note: *brucite; #gibbsite.

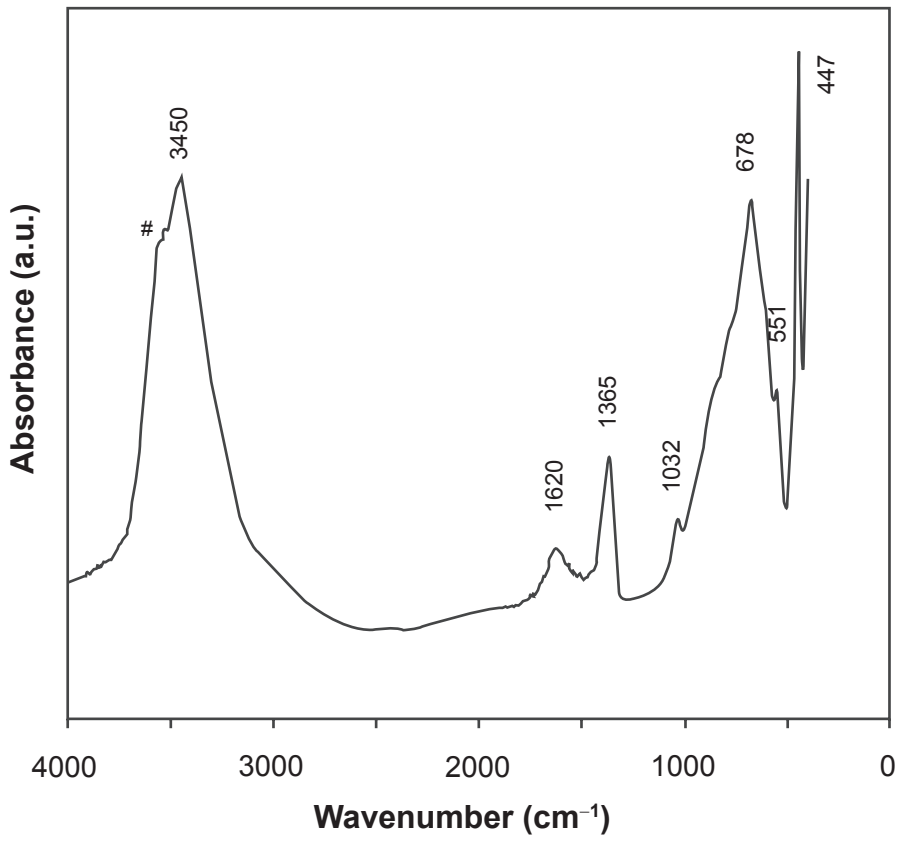

Figure 2 FTIR spectrum of pristine Mg_2Al-Cl-LDH nanomaterials. Shoulder with # is characteristic of Mg_2Al-Cl-LDH.

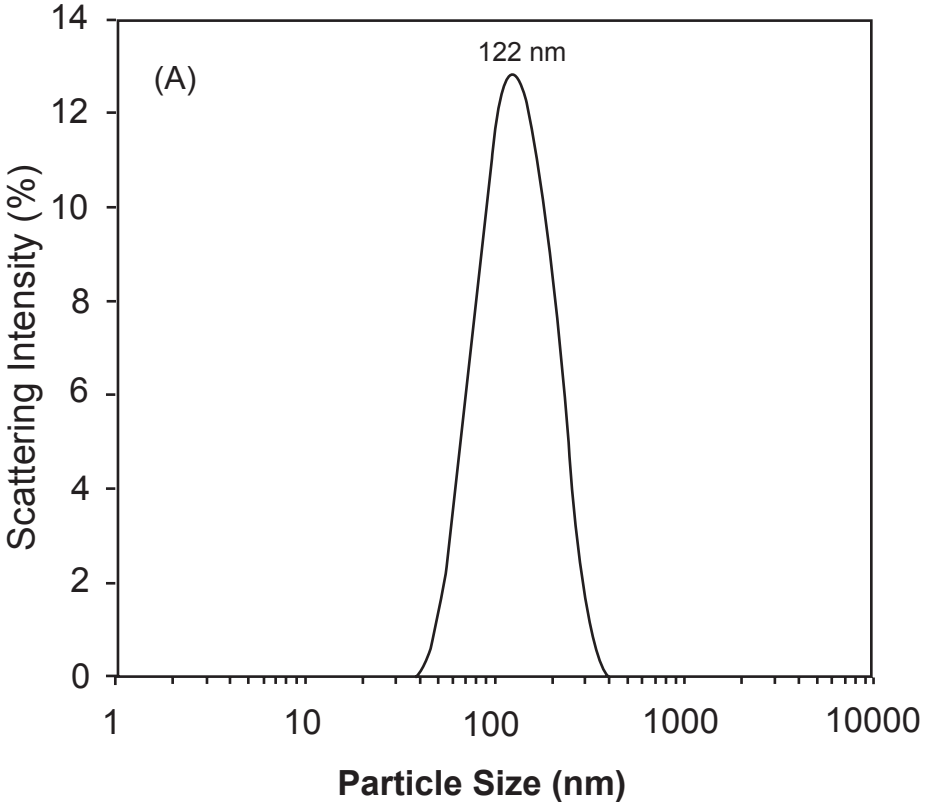

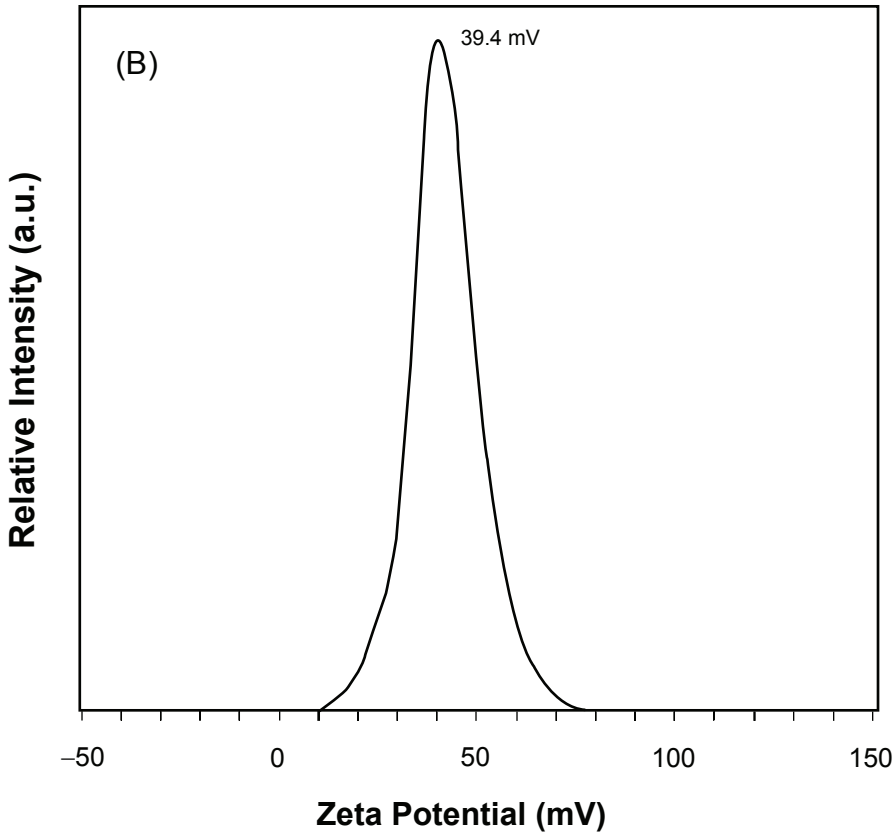

Figure 3 (**A**) Particle size distribution and (**B**) Zeta potential distribution of pristine Mg_2Al-Cl-LDH nanoparticle suspension.

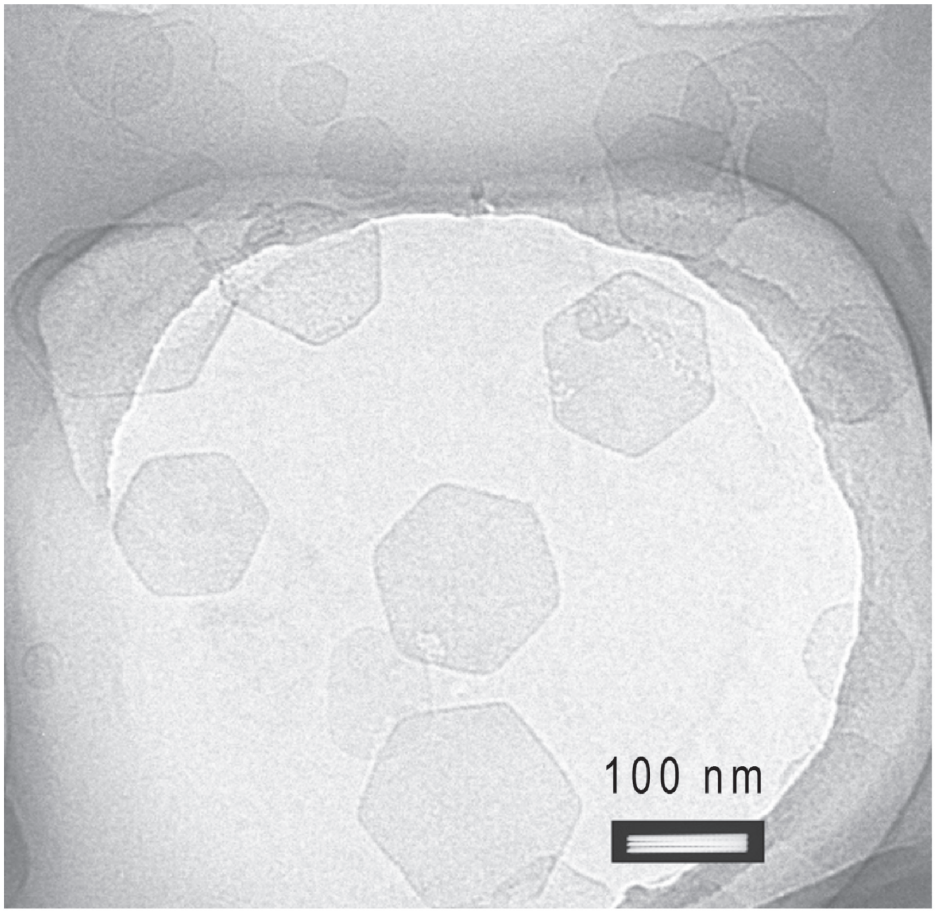

Figure 4 TEM image of typical Mg_2Al-Cl-LDH.

dimension in 50–150 nm from this image. These hexagonal nanoplates are well separated from one another, with very limited casual inter-connection. The lateral dimension from TEM images is statistically equivalent to the hydrodynamic diameter from PCS although the thickness is much smaller than the lateral dimension. The thickness of LDH nanoparticles is estimated to be ~15 nm from the full-width-at-half-maximum of XRD diffraction peaks (003) and (006) (Cullity 1978) or 8–16 nm from a few TEM images, giving an aspect ratio of 5–10.

LDH-DNA nanohybrids

When plasmid DNA is added into the MgAl-Cl-LDH suspension, DNA chains should exchange with the chloride anions and intercalate into the LDH interlayer spacing, at least partially. As reported by Desigaux and colleagues (2006), DNA fragments with 100–500 and 6000–8000 base pairs can be intercalated at temperatures from 25 to 60 °C. In the current research, however, the DNA amount is much smaller than that required for the full exchange reaction. For example, in a typical delivery test, 80 μg of plasmid DNA is reacted with 1.0 mL of the LDH suspension which contains 4.0 mg of LDH, ie, the weight ratio of DNA:LDH is 1:50. This means that the added plasmid DNA can only exchange 1.5% Cl^- in LDH theoretically[1]. Such a small portion of DNA-LDH hybrids could not induce noticeable diffraction in the XRD pattern. However, the addition of DNA to the LDH suspension has indeed caused the some LDH nanoparticles to agglomerate into aggregates. As shown in Figure 5A, a large DNA-LDH aggregate recorded with STEM contains a number of LDH nanoparticles, some of which are hexagonally shaped as usual. The aggregates are even visually observable when more DNA is added into the LDH suspension, for example, at DNA:LDH weight ratio up to 1:10. This aggregation could be due to the interactions of the supercoiled plasmid DNA with a few LDH nanoparticles. It is reasonable to assume that the supercoiled plasmid size is at least 200–300 nm (Ma and Bllomfield 1994; Marko and Siggia 1995). Therefore, one DNA supercoil

[1]The ratio of DNA negative charges over Al (2[b.p.]/[Al]) is roughly 1.5:100 when the weight ratio of DNA/LDH is 1:50 as an average base pair molecular weight is 660 with two negative charges and LDH has molecular weight of 250 with one positive charge.

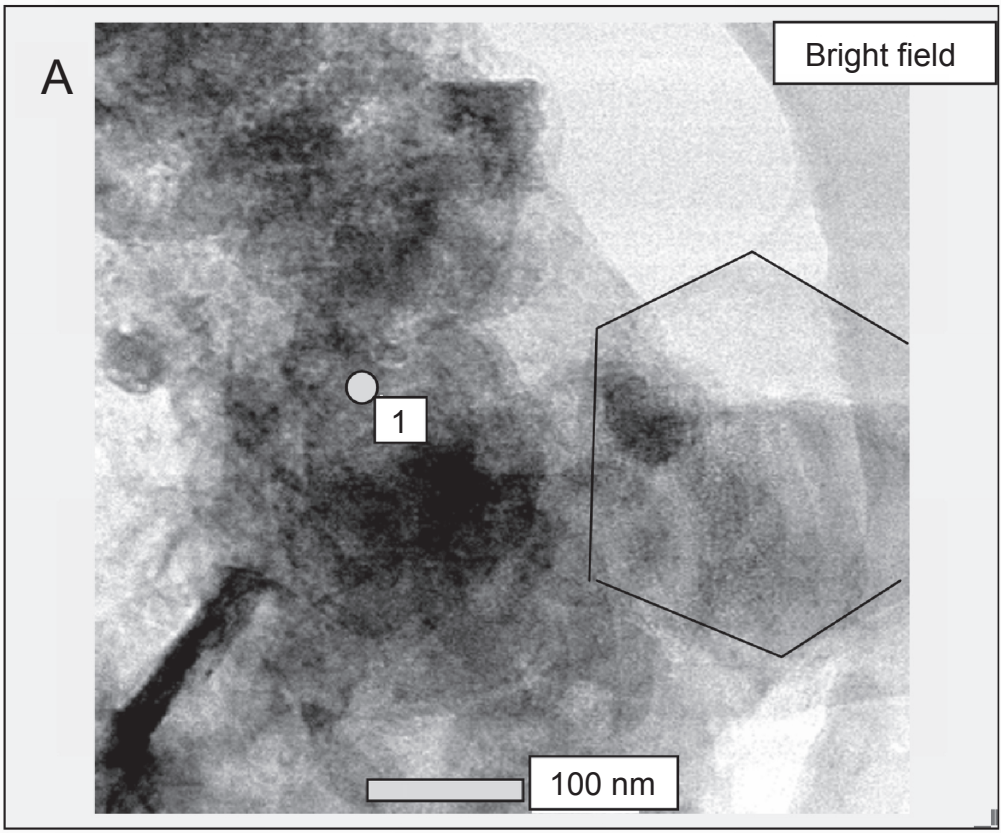

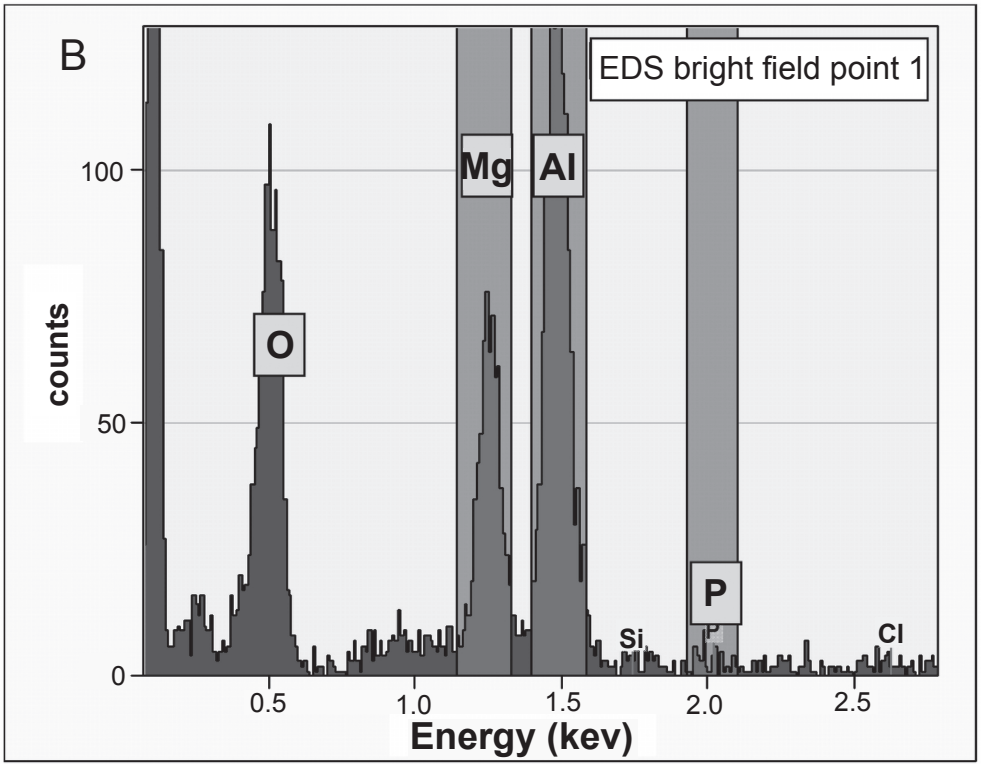

Figure 5 (**A**) STEM image and (**B**) EDX spectrum of DNA-LDH nanohybrids.

cannot be intercalated into only one LDH nanoparticle (about 100 nm), ie, some parts of DNA fragment must be outside of this LDH nanoparticle. These parts may be simply exposed to aqueous solution, but more likely, intercalated into other LDH nanoparticles due to its high affinity for LDH via electrostatic interactions (Desigaux et al 2006). Thus, a few LDH nanoparticles interconnected by the DNA supercoil can lead to the formation of a big aggregate.

In addition, the element analysis for the marked dot (Figure 5A), based on the STEM EDS spectrum (Figure 5B), first indicates the existence of Mg (1.2 keV) and Al (1.5 keV) in considerable amount. The phosphorus element, only attributed to the DNA chain, is detected in a marginal amount at around 2 keV in the EDS spectrum, possibly showing the existence of the plasmid DNA that is embedded within this aggregate.

Cytotoxicity of LDH nanomaterials

The viability of HEK 293T cells in the presence of Mg_2Al-Cl-LDH nanomaterial at various concentrations is shown in Figure 6. Mg_2Al-Cl-LDH has a lower degree of cytotoxicity although it gives an obvious decrease in cell viability after 2 days at a concentration over 200 μg/mL. 50% cell viability occurs at a concentration of around 500 μg/mL. As expected, increase in the LDH concentration leads to higher cell death. For example, at 1000 μg/mL of LDH only *ca*. 30% HEK 293T cells are viable and almost 100% cell death is observed at 2000 μg/mL of LDH. This observation conflicts with the report by Choy et al. who claim that Mg_2Al-LDH at 1000 μg/mL does not affect the viability of HL-60 cells (Kriven et al 2004). This difference may indicate that LDH material shows variable toxicity in different cell lines. In addition, the slightly higher Mg^{2+} concentration in the buffer (2mM $MgCl_2$ and 1mM $AlCl_3$) may have additional toxic effects on cells in our tests.

We have noted that Mg_2Al-LDH at concentration of 200–500 μg/mL causes some cell death. However, this concentration is much higher than the concentration (50–100 μg/mL) used in our gene delivery tests, indicating LDH is a safe material for the gene delivery. In comparison, LDH has a much lower cytotoxicity than polymeric materials. For example, 10 μg/mL of PEI can cause 50% cell death (Choi et al 2004). Therefore, if LDH has a transfection efficiency higher than or comparable with that of polymeric materials, LDH should be a more appropriate and promising system for the gene delivery.

Although the exact mechanism of the cytotoxicity is not well understood, it is believed that this is due in part to membrane disruption. As reported by Sayes et al for the cytotoxicity of C_{60} (Sayes et al 2004, 2005), C_{60} leads to lipid peroxidation and therefore disrupts the cell membrane (Chen et al 2005). As for LDH nanoparticles, the positive charges on the particle surface may bind the nanoparticles to the external membrane, especially at a higher concentration. When the whole cell membrane is covered by LDH nanoparticles and most particles are not internalized, the normal functions of cells may be interrupted, thus causing some irritation or damage to the cell membrane and leading to apoptosis (Rhaese et al 2003). In this regard, not only the composition of LDH nanomaterials, but also the charge density and particle size of LDH nanoparticles are primary factors determining the cytotoxicity. Moreover,

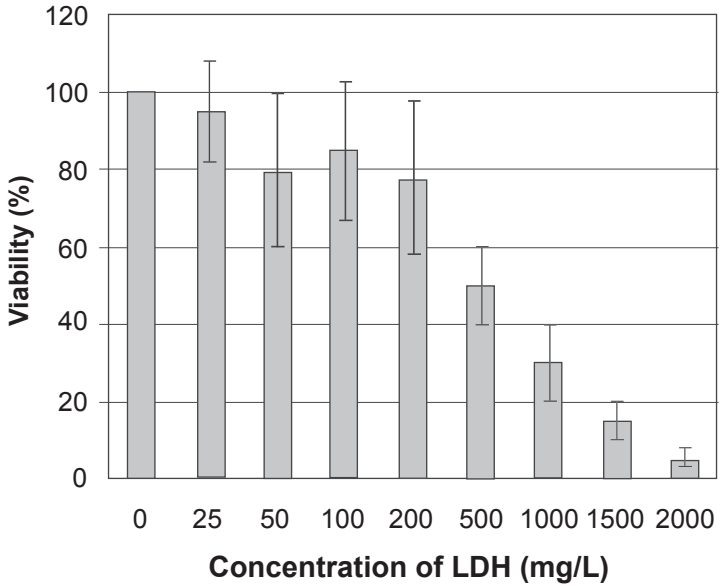

Figure 6 HEK 293 cell viability versus Mg_2Al-Cl-LDH concentration.

the cytotoxicity of LDH nanomaterials on different cell types should also be investigated.

Transfection of HEK 293T cells

DNA-LDH nanohybrid particles were assessed for in vitro transfection efficiency in HEK 293T cells, in comparison with the delivery of naked plasmid DNA and DNA-FuGENE®6 particles where FuGENE®6 is a commercial polymeric transfection reagent. As expected, there is no expression of GFP with naked DNA for 1–3 days at concentrations between 0.25 and 2.0 μg/mL. With LDH nanoparticles as the gene delivery agent, some expression of GFP was evident as fluorescent cells were observed following transfection after 1 day. More fluorescent cells were seen after 2 or 3 days with brighter fluorescence. As shown in Figure 7A, three bright fluorescent HEK 293T cells are observed in this field of view after transfection with LDH at DNA:LDH weight ratio of 1:25 (1.0 μg/mL DNA) after 2 days. The corresponding bright-field image (Figure 7B) indicates most cells are viable. In another batch of tests (DNA:LDH weight ratio was 1:50 and DNA concentration was 1.0 μg/mL), more weakly fluorescing cells were observed 2 days after transfection (Figure 7C). We have also tested the transfection under slightly different conditions. For example, DNA concentration was varied at 0.25, 0.5, 1.0 and 2.0 μg/mL with DNA:LDH weight ratio being 1:25, 1:50 or 1:100. Although visual observation and FACS data (in the following section) have not revealed an optimum condition, it seems that [DNA] = 1.0 μg/mL with DNA:LDH weight ratio of 1:25 leads to better transfection. In these experiments, all individual tests show a similar trend in that cells with more GFP expression and therefore increasing fluorescence intensity are related to the increase in DNA concentration and incubation time up to 3 days (details are given in the next section). Generally, 3 days after transfection, fluorescent cells do not increase in number and there is higher cell death due to the limited supply of nutrition.

As shown in Figure 7D, many more HEK 293T cells are transfected with the commercial agent FuGENE®6 under very similar conditions. Figures 7C and 7D indicate that the transfection efficiency using LDH nanoparticles as the agent is approximately 10% of that using FuGENE®6.

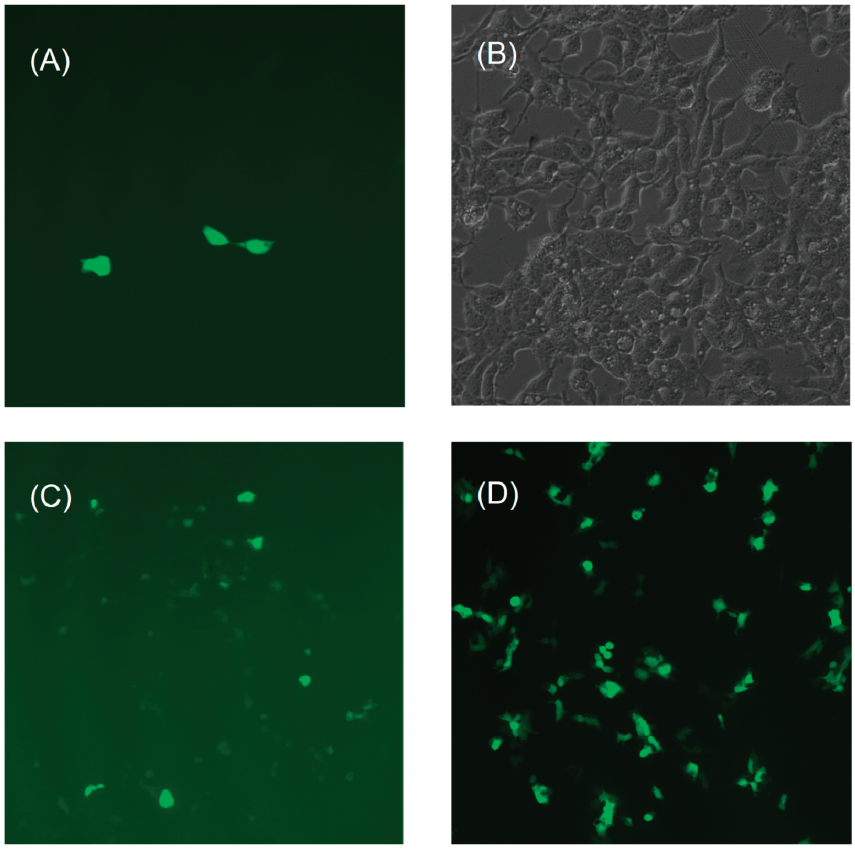

Figure 7 Fluorescence microscopic images of cells with GFP expressed two days after transfection. (**A**) and (**C**): using LDH nanoparticles; (**D**): using the commercial agent FuGENE®6 as transfection agent ([DNA] = 1.0 μg/mL and [FuGENE®6] = 5.0 μg/mL?). (**B**): brightfield image of image (**A**).

FACS analysis

Fluorescence activated flow cytometry was used to measure how many cells express the green fluorescent protein and how much of this fluorescent protein is expressed. The typical fluorescence FACS profiles are shown in Figure 8, separated by the line with fluorescence intensity of 2000, below which the fluorescence is attributed to the background and above which the fluorescence is due to the transfected cells as well as dead cells. Obviously, there are no fluorescent cells in the control experiment (Figure 8A) 2 days after transfection. As expected, the plasmid DNA does not lead to any transfection by itself (Figure 8B). Unexpectedly, some cells (0.6%, Figure 8C) seem to fluorescence at 100 μg/mL of LDH, possibly due to the autofluorescence of dead cells. As shown in Figure 6, the cell viability is slightly reduced at 100 μg/mL of LDH nanoparticles, and thus some dead cells are likely to be present. Further shown in Table 1, there were 0.4%–0.5% cells showing the fluorescence after 1- and 2-day incubation, and thus it is expected that 25 μg/mL of LDH (normally used for DNA delivery in this research) would cause much less cell death, possibly ca. 0.1% of cell population, so the effect of LDH materials on the GFP fluorescence of cells can be ignored for data analysis in these tests. However, 3-day incubation led to much more cell death, largely due to the continuous influence of LDH on cell viability with the limited supply of nutrition.

Using LDH nanoparticles causes a significant increase in the number of fluorescent cells. As shown in Figures 8D–8F, many more dots (cells) are above the line 2 days after transfection with LDH-DNA nanohybrids. As the DNA dose increases from 0.25 to 1.0 μg/mL while LDH concentration is kept at 25 μg/mL, the percentage of fluorescent cells increases from 1.0% to 4.1%. Table 1 shows that the average percentage of GFP-expressed cells increases with the increase in the plasmid DNA concentration in LDH-DNA nanohybrids. This implies that the DNA-LDH hybrids enter into cells in a DNA dose dependent manner (Choy et al 2000). In addition, Table 1 also shows effect of the incubation time. For example, *ca*. 1.13% cells were transfected after 1 day while this percentage increased to 3.95% after day 2 of transfection and then decreased to 3.27% 3 days after transfection at the DNA concentration of 1.0 μg/mL. As the nutrition became limited and the cell confluence was high in the third day, the percentage of fluorescent cells decreased. However, the median fluorescence intensity reaches maximum after day 3.

In summary, the transfection efficiency using LDH nanoparticles as the agent is still relatively low. Our FACS data suggest that the percentage of transfected cells is *ca.* 3%–6% 2 days after transfection. In comparison with the commercial agent FuGENE®6, the number of fluorescent cells are about 10% under the similar conditions, as seen in the images of

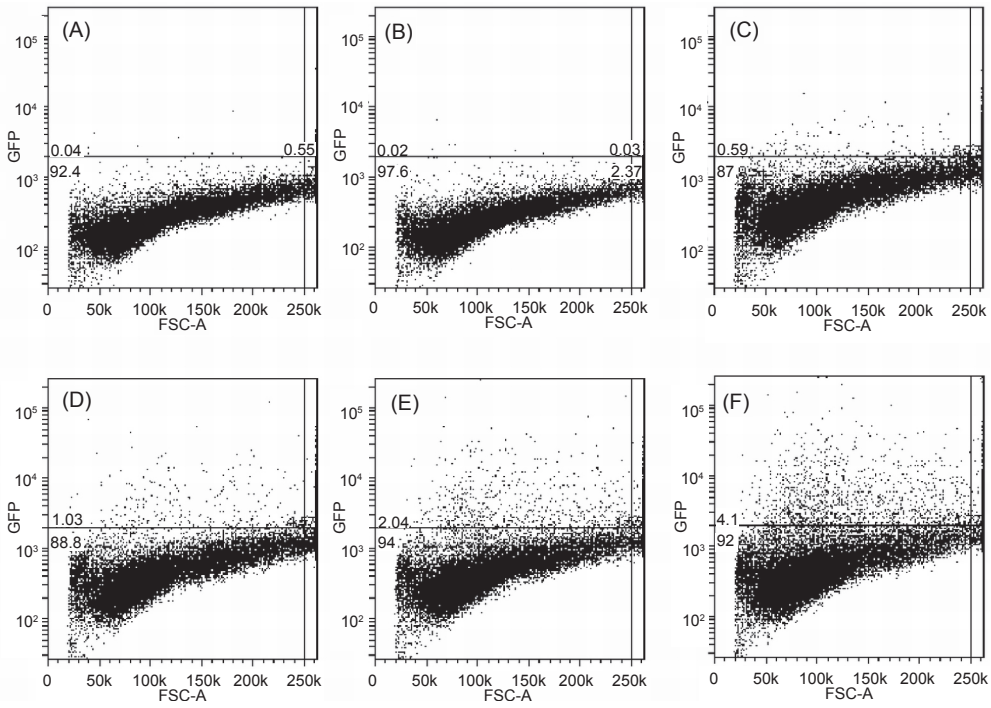

Figure 8 FACS profile of HEK 293T cells with GFP proteins transfected under various conditions. (**A**) Controlled experiment; (**B**) 1.0 μg/mL of plasmid DNA; (**C**) 100 μg/mL of LDHs; (**D**) 0.25 μg/mL of DNA and 25 μg/mL of LDH; (**E**) 0.50 μg/mL of DNA and 25 μg/mL of LDH; (F) 1.0 μg/mL of DNA and 25 μg/mL of LDH.

Table 1 The percentage of GFP-expressing cells (above the gate at fluorescence intensity of 2000 in Figures 8 and 9).

Day	DNA only[a]	LDH only[b]	0.25 μg/mL DNA in LDH-DNA[c]	0.50 μg/mL DNA in LDH-DNA[c]	1.0 μg/mL DNA in LDH-DNA[c]
1	0.10 ± 0.05[d]	0.41 ± 0.10	0.40 ± 0.30	0.77 ± 0.39	1.13 ± 0.58
2	0.04 ± 0.02	0.49 ± 0.19	0.84 ± 0.42	3.23 ± 1.66	3.95 ± 1.48
3	0.04 ± 0.01	1.35 ± 0.50	0.97 ± 0.21	2.18 ± 1.41	3.27 ± 1.45

Note: [a]The plasmid DNA concentration was 1.0 μg/mL in the tests; [b]The LDH concentration was 100 μg/mL in the tests; [c]The plasmid DNA concentration was varied at 0.25, 0.50 and 1.0 μg/mL while the LDH concentration was kept at 25 μg/mL in the tests; [d]The average percentage and standard deviation were calculated from the data in 3 or 4 experiments.

Figures 7C and 7D. This relative transfection efficiency also varies from 7% to 15% with the DNA concentration at 0.25–2.0 μg/mL under similar experimental conditions.

Factors affecting transfection efficiency

The low delivery efficiency may indicate that the barriers for delivery into the cell nucleus, such as the cellular uptake (endocytosis), endosomal escape, dissociation of the plasmid DNA and nuclear trafficking, are not effectively overcome. The main factor causing such low transfection efficiency, in our belief, is DNA-LDH hybrid particle size.

It is suggested that particles less than about 150 nm in diameter are preferred for endocytosis (Prabha et al 2002; Leong 2005). However, as discussed previously, aggregation of LDH nanoparticles in the presence of DNA can lead to the DNA-LDH hybrid particle size of 500–1000 nm (Figure 5A), much bigger than 150 nm. This directly reduces the cellular uptake by endocytosis. In addition, the bigger DNA-LDH aggregates are not well dispersed in the growth medium due to the relatively quick sedimentation, so that some cells in the wells are not readily exposed to the LDH-DNA nanohybrids and have less chance to be transfected. In this regard, LDH nanoparticles seem not suitable for delivering long chain DNA fragments (linear or supercoiled), such as those with more than 1000 base pairs.

In addition, the DNA-LDH nanohybrids have to escape from the endosome after passing through the cell membrane. The DNA-LDH nanohybrids have to then release the plasmid DNA fragment. During these two processes, the parts of the DNA fragment outside of LDH nanoparticles that are exposed to the environment could be attacked by enzymes and degraded (Choy et al 2000). Furthermore, the released naked DNA fragment could also be degraded during its translocation to the nucleus. The liability of gene degradation in these several processes finally reduces the chance for the plasmid DNA to reach the nucleus and be transcribed into GFP mRNA.

Conclusions

Pristine Mg_2Al-Cl-LDH nanoparticles were prepared with the lateral size of 50–300 nm. The positive zeta potential of 39 mV makes it very suitable for cellular uptake. This high positive charge on the LDH surface, however, makes it more likely to adhere to the cell membrane, interfere with cellular functions and cause cell death at high concentrations of LDH materials. The tests for supercoiled pEF-eGFP plasmid delivery indicate that this nanomaterial can be used as a nonviral system for gene delivery, however the delivery efficiency is low under current conditions. Briefly, *ca*. 3%–6% of total cells successfully expressed the GFP protein, corresponding to 7%–15% efficiency of that using the commercial agent FuGENE®6 under similar conditions. The major factor leading to the low efficiency could be attributed to the aggregation of LDH nanoparticles with the long-chain DNA.

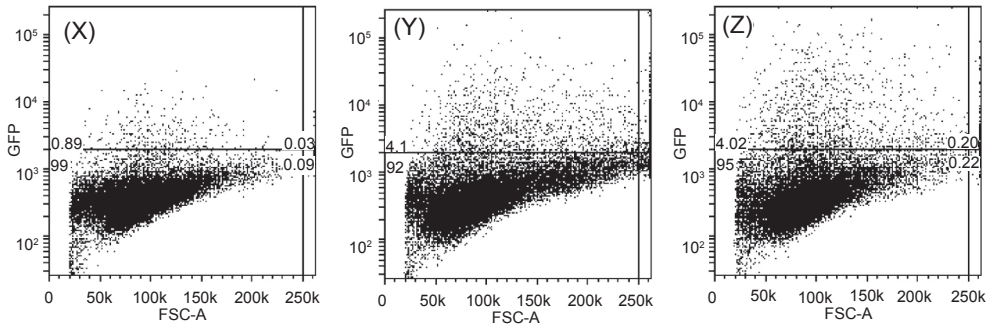

Figure 9 FACS profile of HEK 293T cells with GFP proteins transfected after (**X**) 1 day, (**Y**) 2 days, and (**Z**) 3 days with 1.0 μg/mL of DNA and 25 μg/mL of LDH, respectively.

Acknowledgments

Funding from the Australian Research Council for the Centre of Functional Nanomaterials ARC Discovery project (DP0559594) and UQ Early Career Researcher Grant (2004001428) is gratefully acknowledged.

References

Barbe C, Bartlett J, Kong L, et al. 2004. Silica particles: a novel drug-delivery system. *Adv Mater*, 16:1959–1966.

Boclair JW, Braterman PS. 1999. Layered double hydroxide stability. 1. Relative stabilities of layered double hydroxides and their simple counterparts. *Chem Mater*, 11:298–302.

Braterman PS, Xu ZP, Yarberry F. 2004. Layered double hydroxides. In: Auerbach SM, Carrado KA, Dutta PK, ed. Handbook of layered materials. New York: Marcel Dekker, Inc. p 373–474.

Cai H, Hillier AC, Franklin KR, et al. 1994. Nanoscale imaging of molecular adsorption. *Science*, 266:1551–3.

Cavani F, Trifiro F, Vaccari A. 1991. Hydrotalcite-like anionic clays: preparation, properties and applications. *Catal Today*, 11:173–301.

Chen DJ, Majors BS, Zelikin A, et al. 2005. Structure-function relationships of gene delivery vectors in an limited polycation library. *J Controlled Release*, 103:273–283.

Choi JS, Nam K, Park JY, et al. 2004. Enhanced transfection efficiency of PAMAM dendrimer by surface modification with L-arginine. *J Controlled Release*, 99:445–456.

Choy JH, Kwak SY, Jeong YJ, et al. 2000. Inorganic layered double hydroxide as nonviral vectors. *Angew Chem Int Ed*, 39:4042–5.

Choy JH, Kwak SY, Park JS, et al. 2001. Cellular uptake behaviour of γ-^{32}P labeled ATP-LDH nanohybrids. *J Mater Chem*, 11:1671–4.

Choy JH, Kwak SY, Park JS, et al. 1999. Intercalative nanohybrids of nucleoside monophosphates and DNA in layered metal hydroxides. *J Am Chem Soc*, 121:1399–1400.

Cullity BD. 1978. Elements of x-ray diffraction. Massachusetts: Addison-Wesley.

Desigaux L, Belkacem MB, Richard P, et al. 2006. Self-assembly and characterization of layered double hydroxide/DNA hybrids. *Nano Letters*, 6:199–204.

Dietz GPH and Bahr M. 2004. Delivery of bioactive molecules into the cell: the Trojan horse approach. *Mol Cellular Neurosci*, 27:85–131.

Hernandez-Morento MJ, Ulibarri MA, Rendon JL, et al. 1985. IR characteristics of hydrotalcite-like compounds. *Phys Chem Miner*, 12:34–8.

Khalil IA, Kogure K, Akita H, et al. 2006. Uptake pathways and subsequent intracellular trafficking in nonviral gene delivery. *Pharmacol Review*, 58:32–45.

Kriven WM, Kwak SY, Wallig MA, et al. 2004. Bio-resorbable nanoceramics for gene and drug delivery. *MRS Bulletin*, 29:33–7.

Leong KW. 2005. Polymeric controlled nucleaic acid delivery. *MRS Bulletin*, 30:640–6.

Luo D, Saltzman WM. 2000. Enhancement of transfection by physical concentration of DNA at the cell surface. *Nature Biotech*, 18:893–5.

Ma C, Bllomfield VA. 1994. Condensation of supercoiled DNA induced by $MnCl_2$. *Biophys J*, 67:1678–1681.

Marko JF, Siggia ED. 1995. Statistical mechanics of supercoilde DNA. *Phys Rev E*, 52:2912–2938.

Nakamoto K. 1997. Infrared and Raman spectra of inorganic and coordinate compounds. John New York:Wiley & Sons, Inc.

Nielsen PE. 2005. Systemic delivery: the last hurdle? *Gene Ther*, 12:956–7.

Pouton CW, Seymour LW. 1998. Key issues in non-viral gene delivery. *Adv Drug Delivery Review*, 34:3–19.

Prabha S, Zhou WZ, Panyam J, et al. 2002. Size-dependency of nanoparticle-mediated gene transfection: studies with fractionated nanoparticles. *Inter J Pharm*, 244:105–115.

Rhaese S, von Briesen H, Rubsamen-Waigmann H, et al. 2003. Human serum albumin polyethylenimine nanoparticles for gene delivery. *J Controlled Release*, 92:199–208.

Sayes CM, Fortner JD, Guo W, et al. 2004. The differential cytotoxicity of water-soluble fellerenes. *Nano Letters*, 4:1881–4.

Sayes CM, Gobin AM, Ausman KD, et al. 2005. Nano-$C6_0$ cytotoxicity is due to lipid peroxidation. *Biomaterials*, 26:7587–7595.

Tyner KM, Roberson MS, Berghorn KA, et al. 2004. Intercalation, delivery, and expression of the gene encoding green fluorescence protein utilizing nanobiohybrids. *J Controlled Release*, 100:399–409.

van der Aa, MAEM, Mastrobattista E, Oosting RS, et al. 2006. The nuclear pore complex: the gateway to successful nonviral gene delivery. *Pharm Research*, 23:447–459.

Xu ZP, Zeng QH, Lu, GQ, et al. 2006a. Inorganic nanoparticles as carriers for efficient cellular delivery. *Chem Eng Sci*, 61:1027–1040.

Xu ZP, Stevenson G, Lu CQ, et al. 2006b. Stable suspension of layered double hydroxide nanoparticles in aqueous solution. *J Am Chem Soc*, 128:36–37.

Xu ZP, Zeng HC. 2001. Abrupt structural transformation in hydrotalcite-like compounds $Mg_{1-x}Al_x(OH)_2(NO_3)_x$ nH_2O as a continuous function of nitrate anions. *J Phys Chem B*, 105:1743–9.